Degradation of the insecticide propoxur by electrochemical advanced oxidation processes using a boron-doped diamond/air-diffusion cell

Diego R. V. Guelfi[1], Fábio Gozzi[1], Ignasi Sirés[2], Enric Brillas[2], Amílcar Machulek Junior[1], Silvio César de Oliveira[1]*

[1]*Instituto de Química (INQUI), Universidade Federal de Mato Grosso do Sul, Av. Senador Filinto Muller, 1555, Caixa postal 549, MS 79070-900 Campo Grande, Brazil*

[2]*Laboratori d'Electroquímica dels Materials i del Medi Ambient, Departament de Química Física, Facultat de Química, Universitat de Barcelona, c/ Martí i Franquès 1-11, 08028 Barcelona, Spain*

*Corresponding Author:

Tel.: +55 6733453551; Fax: +55 6733453552

E-mail address: scolive@gmail.com (S.C. de Oliveira)

1

1   **Abstract**   A solution with 0.38 mM of the pesticide propoxur (PX) at pH 3.0 has been

2   comparatively treated by electrochemical oxidation with electrogenerated H_2O_2 (EO-H_2O_2),

3   electro-Fenton (EF) and photoelectro-Fenton (PEF). The trials were carried out with a 100 mL

4   boron-doped diamond (BDD)/air-diffusion cell. The EO-H_2O_2 process had the lowest

5   oxidation ability due to the slow reaction of intermediates with $^\bullet$OH produced from water

6   discharge at the BDD anode. The EF treatment yielded quicker mineralization due to the

7   additional $^\bullet$OH formed between added Fe^{2+} and electrogenerated H_2O_2. The PEF process was

8   the most powerful since it led to total mineralization by the combined oxidative action of

9   hydroxyl radicals and UVA irradiation. The PX decay agreed with a pseudo-first-order

10   kinetics in EO-H_2O_2, whereas in EF and PEF it obeyed a much faster pseudo-first-order

11   kinetics followed by a much slower one, which are related to the oxidation of its Fe(II) and

12   Fe(III) complexes, respectively. EO-H_2O_2 showed similar oxidation ability within the pH

13   range 3.0-9.0. The effect of current density and Fe^{2+} and substrate contents on the

14   performance of the EF process was examined. Two primary aromatic products were identified

15   by LC-MS during PX degradation.

18

1   **Introduction**

2   The identification of pesticide residues and other highly hazardous chemicals in surface

3   water, groundwater, drinking water and other natural aqueous matrices highlights the

4   ineffectiveness of traditional water management approaches to remove persistent organic

5   pollutants (POPs) (Biziuk et al. 1996; Borràs et al. 2010). The presence of these residues in

6   drinking water and food is associated with a worrisome propagation of various diseases in

7   human beings (Pimentel 1996; Chiron et al. 2000). The pesticide propoxur (PX, $C_{11}H_{15}NO_3$,

8   2-isopropoxyphenyl-*N*-methylcarbamate) is used as a carbamate insecticide since it was

9   introduced in the market in 1959 by Bayer under the trade name Baygon[®]. It is classified as a

10 highly toxic compound by the World Health Organization and the Brazilian Health

11 Surveillance Agency (WHO 2003; ANVISA 2015). PX is used to control a variety of insect

12 pests in public health, agricultural and veterinary medicine applications. It is a potential

13 contaminant of the aquatic environment and food sources due to its high solubility in water,

14 likely to be moderately persistent and mobile in soils (Pérez-Ruiz et al. 2007; Pandey and Guo

15 2014). In Brazil, for instance, PX has been detected at levels up to 10 ng L^{-1} in surface water

16 from coffee crops (Soares et al. 2013).

17   Due to the widespread use of pesticides, there is a growing need to develop potent

18 treatment methods for their removal from contaminated sites. Within this framework, the

19 advanced oxidation processes (AOPs), which rely on the oxidation of pollutants by in situ

20 generated reactive oxygen species (ROS) like hydroxyl radical ($^{\bullet}$OH), have attracted great

21 interest. The high standard reduction potential of this radical ($E^{\circ} = 2.8$ V/SHE) favors its non-

22 selective reaction with many organic compounds up to their mineralization, i.e., conversion

23 into CO_2, H_2O and inorganic ions (Panizza and Cerisola 2009; Sirés and Brillas 2009;

24 Machulek Jr. et al. 2013; Vasudevan and Oturan 2014). A large variety of AOPs has been

3

applied to degrade pesticides, including photocatalysis (Ramos et al. 2015; Reddy and Kim 2015), ozone (Machulek Jr. et al. 2009; Gozzi et al. 2012; Reddy and Kim 2015), Fenton and photo-Fenton (Rao and Chu 2010; Gozzi et al. 2012; Reddy and Kim 2015) and electrochemical AOPs (EAOPs) (Rodrigo et al. 2014). However, only few works have described the removal of PX from water, based on heterogeneous photocatalysis (Lu et al. 1999; Sanjuán et al. 2000; Mahalakshmi et al. 2009) and ozone (Benítez et al. 1995), but there are no previous studies reporting its degradation by EAOPs.

Over the last two decades, several EAOPs like electrochemical oxidation (EO), electro-Fenton (EF) and photoelectro-Fenton (PEF) have emerged as promising, simple and versatile solutions that can be easily adapted to the treatment of organics contained in wastewater (Brillas et al. 2009; Klavarioti et al. 2009; Sirés et al. 2014; Brillas and Martínez-Huitle 2015). The most common EAOP is EO, in which organic pollutants are directly destroyed at the surface of the anode M and/or by physisorbed hydroxyl radical (M($^\bullet$OH)) formed from water oxidation at high applied current via reaction (1) (Marselli et al. 2003; Martínez-Huitle and Ferro 2006; Panizza and Cerisola 2009).
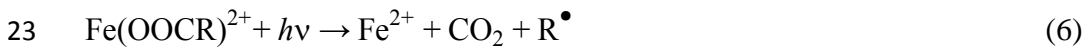
$$M + H_2O \rightarrow M(^\bullet OH) + H^+ + e^- \tag{1}$$

The oxidation ability of EO depends on the anode used. Boron-doped diamond (BDD) films have demonstrated their superiority over classical anodes such as Pt and PbO_2 (Ciríaco et al. 2009; Guinea et al. 2009; Rodrigo et al. 2010; Cavalcanti et al. 2013), owing to their extremely wide potential window, inert surface, slight BDD-$^\bullet$OH interaction and larger O_2-overpotential, thereby enhancing the reaction of $^\bullet$OH with organics (Panizza and Cerisola 2009; Sirés et al. 2014).

When EO is performed with a cathode that allows the continuous electrogeneration of H_2O_2 from the two-electron reduction of O_2 gas by reaction (2), the process is called EO-

4

H$_2$O$_2$. Examples of efficient cathode materials for this purpose include graphite felt (Vatanpour et al. 2009), carbon nanotubes (Khataee et al. 2014), carbon felt (Dirany et al. 2012; El-Ghenymy et al. 2014; Yahya et al. 2014), carbon-polytetrafluoroethylene (PTFE) (Borràs et al. 2010; Thiam et al. 2014, 2015) and BDD (Cruz-González et al. 2012). In EO-H$_2$O$_2$ with a BDD anode, organics are preferentially destroyed by physisorbed BDD($^\bullet$OH), with minor participation of other ROS such as H$_2$O$_2$ and its anodic oxidation product HO$_2^\bullet$ (Sirés and Brillas 2012).

$$O_{2(g)} + 2H^+ + 2e^- \rightarrow H_2O_2 \qquad (2)$$

EF involves the addition of a small amount of Fe^{2+} as catalyst to upgrade the oxidation ability of cathodically generated H$_2$O$_2$. Thus, via Fenton's reaction (3), Fe^{3+} and $^\bullet$OH are produced in the bulk at optimum pH about 3 (Dirany et al. 2012; El-Ghenymy et al. 2014; Thiam et al. 2014, 2015). BDD($^\bullet$OH) and $^\bullet$OH are then the main oxidizing ROS in EF. Reaction (3) is catalytic because it can be propagated by Fe^{2+} regeneration via reaction (4). The oxidation power of EF can be enhanced in PEF by irradiating the solution with artificial UVA light that causes: (i) the photoreduction of Fe(OH)$^{2+}$, the predominant Fe^{3+} species at pH $\sim$ 3, to Fe^{2+} and $^\bullet$OH by reaction (5) and (ii) the photodecarboxylation of complexes of Fe(III) with carboxylic acids generated from aromatics and heteroaromatics degradation by reaction (6) (Ruiz et al. 2011; Moreira et al. 2013; Florenza et al. 2014; Thiam et al. 2015, 2016).

$$H_2O_2 + Fe^{2+} \rightarrow Fe^{3+} \; ^\bullet OH + OH^- \qquad (3)$$

$$Fe^{3+} + e^- \rightarrow Fe^{2+} \qquad (4)$$

$$Fe(OH)^{2+} + h\nu \rightarrow Fe^{2+} + {}^\bullet OH \qquad (5)$$

$$Fe(OOCR)^{2+} + h\nu \rightarrow Fe^{2+} + CO_2 + R^\bullet \qquad (6)$$

1   This paper presents a comparative study on the degradation of PX solutions by EO-H$_2$O$_2$,

2   EF and PEF using an undivided BDD/air-diffusion cell. The effect of pH on the performance

3   of the EO-H$_2$O$_2$ process was examined. The influence of current density (j) and Fe^{2+} and PX

4   concentrations on the oxidation ability of EF was clarified to assess the role of generated

5   hydroxyl radicals. The decay of the pesticide was followed by high-performance liquid

6   chromatography (HPLC) and the coupling of this technique with mass spectrometry (LC-MS)

7   led to the identification of its primary products.

8   **Experimental details**

9   Chemicals

10   Propoxur (99% purity) was supplied by Sigma-Aldrich. Concentrated hydrogen peroxide

11   (30% w/v), heptahydrated Fe(II) sulfate and anhydrous sodium sulfate were of analytical

12   grade purchased from Vetec Quimica Fina. All the solutions were prepared using ultrapure

13   water from a Millipore Milli-Q system with resistivity > 18 MΩ cm at 25 °C. The initial pH

14   was adjusted to 3.0 by addition of analytical grade sulfuric acid supplied by Vetec Quimica

15   Fina. HPLC grade acetonitrile and other analytical grade chemicals used for analysis were

16   purchased from Vetec Quimica Fina.

17   Electrolytic system

18   The electrolytic experiments were carried out with an open and undivided cylindrical

19   glass cell of 150 mL capacity with a double jacket for circulation of external thermostated

20   water to regulate the solution temperature at 25 ℃. The treated solution was always

21   vigorously stirred with a magnetic bar at 800 rpm for homogenization and for ensuring

22   reactants transport toward/from the electrodes. The anode was a BDD thin-film electrode

supplied by NeoCoat (La-Chaux-de-Fonds, Switzerland) and synthesized by the hot filament

chemical vapor deposition technique on single-crystal p-type Si (100) wafers (0.1 Ω cm,

Siltronix). The cathode was a carbon-PTFE air-diffusion electrode supplied by E-TEK

(Somerset, NJ, USA). It was mounted as described elsewhere (Isarain-Chávez et al. 2010) and

was fed with compressed air at 1 L h^{-1} for continuous H$_2$O$_2$ generation. The geometric area of

both electrodes in contact with the solution was 3 cm^2 and the interelectrode gap was about 1

cm. All the trials were performed at constant j provided by an Instrutherm Fa-3003 power

source. For PEF, the solution was irradiated with a Philips TL/4W/08 fluorescent black light

blue tube of λ_{max} = 360 nm placed at the top of the open cell at 6 cm above the solution. An

incident photon intensity of 2.92 $\times$ 10^{19} photon s^{-1} was determined by standard potassium

ferrioxalate actinometry (Hatchard and Parker 1956). Cleaning of BDD surface and activation

of the air-diffusion cathode were made before electroyses from their polarization in 100 mL

of a 0.05 M Na$_2$SO$_4$ solution at 100 mA cm^{-2} for 180 min.

Solutions of 100 mL with 0.38 mM PX and 0.05 M Na$_2$SO$_4$ were comparatively treated

by EO-H$_2$O$_2$, EF and PEF at pH 3.0 and j = 100 mA cm^{-2}. For the two latter EAOPs, 0.50 mM

Fe^{2+} was added to the solution as catalyst since this content has been usually found as optimal

for many organics degraded under similar conditions (Ruiz et al. 2011; Moreira et al. 2013;

Florenza et al. 2014; Thiam et al. 2015). The influence of pH in the range of 3.0-9.0 on the

oxidation power of EO-H$_2$O$_2$ was investigated. The effect of j in the range 33.3-100 mA cm^{-2},

the initial Fe^{2+} concentration between 0.10 and 1.5 mM and the initial insecticide content

between 0.19 and 0.76 mM on the performance of EF was examined as well.

Instruments and analytical procedures

The solution pH was measured with a Crison 2000 pH-meter. The PX decay was

monitored by reversed-phase HPLC using a Thermo Scientific Finnigan Surveyor system

7

1 equipped with a diode array detector set at $\lambda = 274$ nm. It was fitted with an Agilent

2 Technologies Zorbax Eclipse XDB-C-18 5 μm, 250 mm × 4.6 mm, column. For this

3 analysis, all the samples withdrawn from electrolyzed solutions were filtered with

4 Whatman 0.45 μm PTFE filters, and for EF and PEF, they were previously diluted (1:1)

5 with acetonitrile to stop the degradation process. 25 μL aliquots were injected into the LC

6 and a 60:40 acetonitrile/water mixture at 0.6 mL min^{-1} was eluted as mobile phase. In this

7 technique, the limit of quantification (LOQ) was 0.097 mg L^{-1} and the limit of detection

8 (LOD) was 0.029 mg L^{-1}. Ammonium ion was determined by standard method SM 4500-

9 NH$_3$ C (titrimetric method), with a preliminary distillation step (method B), whereas

10 nitrate ion was determined by standard method SM 4500-NO$_3^-$ E (ALPHA, 2012). The

11 LOQ and LOD for these analyses were 0.100 mg L^{-1} and 0.032 mg L^{-1}, respectively.

12 For the mineralization analyses, the samples were withdrawn at regular times, filtered

13 with Whatman 0.45 μm PTFE filters and their total organic carbon (TOC) content was

14 determined immediately on a Shimadzu TOC-V CPN analyzer. Reproducible TOC values

15 with ±1% accuracy were found by injecting 50 μL aliquots into the above analyzer, with

16 LOQ = 0.180 mg L^{-1} and LOD = 0.053 mg L^{-1}. These data were then utilized to estimate

17 the mineralization current efficiency (MCE) for each assay at current I (in A) and time t

18 (in h) from Eq. (7) (Isarain-Chávez et al. 2010; Ruiz et al. 2011):

19 $$\text{MCE (\%)} = \frac{n\,F\,V\,\Delta(\text{TOC})_{\text{exp}}}{4.32 \times 10^7\,m\,I\,t} \times 100 \qquad (7)$$

20 where F is the Faraday constant (96,487 C mol^{-1}), V is the solution volume (in L),

21 $\Delta(\text{TOC})_{\text{exp}}$ is the experimental TOC abatement (in mg L^{-1}), 4.32×10^7 is a conversion

22 factor (3,600 s h^{-1} × 12,000 mg C mol^{-1}) and m is the number of carbon atoms of PX (11 C

23 atoms). The number of electrons n involved in the theoretical overall mineralization

24 process of PX was 58 from reaction (8), considering the conversion into carbon dioxide

8

1   and nitrate as pre-eminent ion, as will be discussed below.

2    $C_{11}H_{15}NO_3 + 22H_2O \rightarrow 11CO_2 + NO_3^- + 59H^+ + 58e^-$ (8)

3   The electrolytic experiments were made in duplicate with good reproducibility. In all

4   cases, average results are given with standard deviations lower than 2%.

5   The primary products formed during the EF treatment of 100 mL of a 0.38 mM PX

6   solution at 100 mA cm^{-2} after different electrolysis times were detected by LC-MS. To do

7   this, the organic components of the remaining solutions were extracted with 25 mL of CH_2Cl_2

8   in three times. The organic fractions were mixed, dried over anhydrous Na_2SO_4, filtered and

9   evaporated to dryness on a rotary evaporator. Further, the residue was dissolved in 10 mL of

10   acetonitrile and the resulting solution was analyzed by LC-MS. This was made with the above

11   HPLC system coupled with a Thermo Scientific LCQ Fleet plus system MS. The MS

12   consisted of an ESI source operated in positive mode, at a spray voltage of 4.5 kV and

13   capillary voltage of 35 V with temperature controlled at 250 ºC. The sheath and auxiliary

14   gases (N_2) flow rates were set at 40 and 10, arbitrary unit, respectively. Mass spectra were

15   collected in the *m/z* range 50-600 using total IC. The analysis was performed by injecting 25

16   μL samples, previously filtered with a Millipore filter of 0.22 μm, into the LC, using a 60:40

17   acetonitrile/water (0.1% acetic acid) mixture at 0.3 mL min^{-1} as mobile phase.

18   **Results and discussion**

19   Comparative degradation of propoxur by EO-H_2O_2, EF and PEF

20   A photostability test was initially made with 100 mL of 0.38 mM (50 mg L^{-1} TOC) PX

21   solutions in 0.05 M Na_2SO_4 at pH 3.0 under UVA irradiation for 120 min. No change in the

22   PX content was found by reverse-phase HPLC, indicating that the herbicide was not

23   photosensitive. The same results were obtained by illuminating the above PX solution in the

9

1   presence of 0.50 mM Fe^{2+} or Fe^{3+}. This points to consider that the possible Fe(II) or Fe(III)

2   complexes of the herbicide are not photoactive under the present experimental conditions.

3   A first series of electrochemical assays was performed by treating 0.38 mM PX solutions

4   in 0.05 M of Na_2SO_4 of pH 3.0 by $EO-H_2O_2$, EF and PEF using a stirred BDD/air-diffusion

5   cell at $j = 100$ mA cm^{-2} and 25 ℃ in order to test the relative oxidation ability of these

6   EAOPs. In EF and PEF, 0.50 mM Fe^{2+} was added as catalyst to the starting solution. Fig. 1

7   depicts the abatement of PX concentration with electrolysis time for these runs. The pesticide

8   disappeared after 300 min of $EO-H_2O_2$, 120 min of EF and 60 min of PEF. The slower decay

9   in $EO-H_2O_2$ can be accounted for by the low reactivity of PX with BDD(•OH) originated from

10   reaction (1). The faster removal in EF is due to the additional oxidation with •OH produced in

11   the bulk from Fenton's reaction (3). The quicker PX decay in PEF can then be related to the

12   generation of more •OH via the photoreduction reaction (5).

13   The above concentration decays were fitted to pseudo-first-order kinetic equations, as

14   shown in the inset panel of Fig. 1. A good straight line was obtained up to 300 min of EO-

15   H_2O_2, as expected if the pesticide reacts with a constant amount of BDD(•OH) during that

16   time (Borràs et al. 2010; Sirés et al. 2014). In contrast, the kinetics in EF and PEF showed a

17   complex behavior, which agreed with two consecutive pseudo-first-order profiles, up to 5 min

18   (first region) and at longer time (second region). Note that the second region was only valid

19   up to relatively short times compared with the total time required for PX disappearance,

20   probably due to the interference arising from the simultaneous degradation of its products.

21   This causes a gradual loss of hydroxyl radicals to attack the raw compound, giving rise to the

22   loss of the pseudo-first-order profile. The poor ability of gas-diffusion cathodes to regenerate

23   Fe^{2+} from Fe^{3+} reduction by reaction (4) is well-known and thus, Fe^{3+} rapidly predominates in

24   solution (Sirés and Brillas 2012; Brillas and Martínez-Huitle 2015). Our results suggest that:

25   (i) in the first region of EF and PEF, PX (or rather, its Fe(II) complexes) is rapidly oxidized

by $^{\bullet}OH$ in the bulk, whereas (ii) in the second region, the accumulation of large quantities of Fe(III)-PX complexes decelerates the pesticide removal since they are more slowly attacked by both, BDD($^{\bullet}OH$) and $^{\bullet}OH$.

Tables 1 and 2 summarize the apparent rate constants k_{app} for EO-H_2O_2 and $k_{app,1}$ for the first region of EF and PEF, as well as $k_{app,2}$ for the second region of the two latter treatments, along with the corresponding square regression coefficients (R_i^2). As can be seen, similar $k_{app,1}$ values were obtained for EF and PEF, corroborating the pre-eminent fast oxidation by $^{\bullet}OH$ in their first region. Conversely, $k_{app,2}$ was about 2.7-fold greater for PEF, although these values were 3.7- and 8.8-fold lower compared to the corresponding $k_{app,1}$ ones, respectively. This brings us to consider that in the second region of the PEF process, the additional $^{\bullet}OH$ formed from reaction (5) largely enhances the destruction of refractory Fe(III)-PX complexes if compared with their much slower abatement upon the action of either BDD($^{\bullet}OH$) or the low amounts of $^{\bullet}OH$ formed via Fenton's reaction (3) once the Fe^{2+} concentration has become smaller. The k_{app} value in EO-H_2O_2 was even 1.6-fold lower than the $k_{app,2}$ one in EF, thus confirming the powerful oxidative action of $^{\bullet}OH$ in Fenton systems.

Fig. 2a highlights that the relative oxidation power of the above processes grew in the order EO-H_2O_2 < EF < PEF, i.e., in agreement with the PX decay sequence (see Fig. 1). The experiments were prolonged for 540 min to reach the total mineralization in some case. In EF and PEF, the solution pH remained practically unchanged, whereas in the case of EO-H_2O_2, the pH was near 3 up to 360 min of electrolysis, whereupon it gradually rose up to a final pH $\sim$ 9-10. This is an indication that final basic products are formed in the latter treatment. Fig. 2a evidences a slow TOC abatement for EO-H_2O_2 as a result of the low reactivity of BDD($^{\bullet}OH$), reaching a final mineralization of 90%. A similar partial mineralization was obtained at the end of EF (see Table 2), although TOC was abated much more rapidly up to

240 min because of the most efficient destruction of intermediates by $^{\bullet}$OH in the bulk. Nevertheless, barely oxidizable products were generated at longer time, thus hampering the mineralization process. In PEF, total mineralization was achieved at 420 min due not only to the efficient removal of products by $^{\bullet}$OH, as in EF, but also to the additional photo-oxidation of intermediates and/or their Fe(III) complexes by UVA light (Thiam et al. 2015, 2016). This finding allows inferring that PEF is the best EAOP for the remediation of wastewater polluted with PX since the combined action of hydroxyl radicals and UVA light is able to completely mineralize all its oxidation products.

At the end of the above EF treatment, a NO_3^- concentration of 0.274 mM (72% of initial N) and NH_4^+ concentration of 0.01 mM (2.6% of initial N) were found, which agrees with the mineralization reaction (8). The MCE values for the trials of Fig. 2a were then calculated from Eq. (7) and the results obtained are given in Fig. 2b. Relevant MCE data are also listed in the two last columns of Table 2. In all cases, the current efficiency decreased progressively with prolonging electrolysis due to two main reasons: (i) the decrease in organic matter content as the degradation proceeds, and (ii) the formation of more recalcitrant products (Panizza and Cerisola 2009; Sirés et al. 2014). As expected, greater MCE values were obtained as the oxidation ability of the EAOP increased. The most powerful PEF process then yielded the highest current efficiency of 12.6% at 30 min.

Effect of pH on the EO-H_2O_2 treatment

It is well known that the oxidation power of EO is frequently dependent on solution pH because of the different reactivity of the acid, neutral and basic forms of organic pollutants with hydroxyl radicals (Panizza and Cerisola 2009). Aiming to improve the oxidation ability of EO-H_2O_2, solutions with 0.38 mM PX in 0.05 M Na_2SO_4 were comparatively treated at initial pH of 3.0, 5.0 and 9.0 using a stirred BDD/air-diffusion cell at j = 100 mA cm^{-2} and 25

12

1 ºC for 540 min. For the two latter cases, no significant pH change was observed up to 420 min

2 but, at longer time, the solutions became more alkaline, with final values near 7 and 10,

3 respectively. This suggests the formation of very recalcitrant basic products at the end of EO-

4 H_2O_2, as discussed above at pH 3.0.

5 Fig. 3a shows a quite similar PX concentration decay regardless of the initial pH,

6 disappearing in 300 min in all cases. This is not surprising taking into account that the neutral

7 form of the pesticide ($pK_a = 12.3$ for deprotonation of its –NH- group to $-N^-$) is the

8 electroactive species in all the pH range under study, not undergoing apparent hydrolysis in

9 weak alkaline medium (Sun and Lee 2003; Mahalakshmi et al. 2009). The inset panel of Fig.

10 3a shows the good pseudo-first-order profiles obtained up to 240-300 min of electrolysis at

11 pH 3.0 and 5.0. At pH 9.0, however, an excellent correlation was only found during the first

12 60 min of treatment because the pesticide abatement was slowed down, probably as a result of

13 a more preferential reaction between BDD($^{\bullet}$OH) and reaction products. From the data of

14 Table 1, one can conclude that the average k_{app} value under these conditions was 0.013 ± 0.03

15 min^{-1}.

16 The TOC-time plots for the above trials, given in Fig. 3b, show quite similar TOC decays

17 in the early and late stages of the treatment, always attaining 90% mineralization as maximal.

18 Table 1 also shows analogous MCE values that varied from 3.7-3.8% at 30 min to 2.1-2.3 at

19 420 min for all these assays. However, the intermediates were more rapidly destroyed at

20 initial pH values of 5.0 and 9.0 from 60 min of treatment, and uniquely the accumulation of

21 very recalcitrant products from 300 min inhibited the mineralization process in such media,

22 therefore reaching the same mineralization degree as that at pH 3.0 at 540 min. Although

23 these results indicate that pH modification did not improve the oxidation power of EO-H_2O_2

24 after prolonged electrolyses, it should be remarked that the trend of TOC decay at initial pH

25 9.0 was quite similar to that of the EF process at pH 3.0 (see Fig. 1). This is very interesting

13

1   from an application standpoint, since EO-H_2O_2 could be used to treat wastewater with PX at

2   pH $\geq$ 5, when EF and PEF cannot be applied.

3   Influence of current density on the EF process
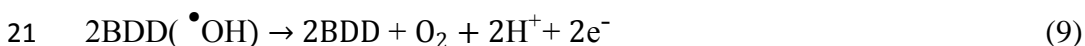
4   To clarify the role of BDD($^\bullet$OH) and $^\bullet$OH originated in Fenton systems, the effect of a

5   key operation parameter such as j on the performance of EF was firstly examined. This

6   parameter determines the amounts of hydroxyl radicals produced and its increase is expected

7   to accelerate the electrode reactions, originating greater quantities of BDD($^\bullet$OH) from

8   reaction (1) and of H_2O_2 from reaction (2), which in turn yields larger amounts of $^\bullet$OH from

9   Fenton's reaction (3) (Sirés et al. 2014; Thiam et al. 2016). The influence of j between 33.3

10   and 100 mA cm^{-2} was assessed by degrading a 0.38 mM PX solution with 0.05 M Na_2SO_4 and

11   0.50 mM Fe^{2+} at pH 3.0 and 25 ºC by EF using the 100 mL BDD/air-diffusion cell.

12   Fig. 4 highlights the expected acceleration of PX removal as a consequence of the higher

13   production of hydroxyl radicals when j grew from 33.3 to 66.6 mA cm^{-2}, disappearing at 180

14   and 120 min, respectively (see Table 2). However, the pesticide decay was similar at 66.6 and

15   100 mA cm^{-2}. This suggests that the electrolytic system is unable to yield higher amounts of

16   reactive BDD($^\bullet$OH) and $^\bullet$OH since the excess of these radicals is consumed to destroy a

17   greater quantity of products and/or in parasitic non-oxidizing reaction. The former possibility

18   was corroborated from the gradually quicker TOC abatement with raising j, as can be

19   observed in Fig. 5a. At the end of these assays, 83%, 88% and 91% mineralization was

20   achieved at 33.3, 66.6 and 100 mA cm^{-2}, respectively (see Table 2).

21   The PX removal always showed two consecutive pseudo-first-order regions for times

22   shorter than 30 min, as can be seen in the inset panel of Fig. 4. The first region only lasted ca.

23   5 min, presenting a very fast pesticide decay due to the main action of $^\bullet$OH onto PX and/or its

24   Fe(II) complexes, with similar $k_{app,1}$ values in all the j range except at 33.3 mA cm^{-2} that led to

14

a slower decrease (see Table 2). Regarding the second region, which was valid from about 5 to 25-30 min, was characterized by a much slower destruction of the herbicide upon attack of BDD($^{\bullet}$OH) and $^{\bullet}$OH onto its Fe(III) complexes, with analogous $k_{app,2}$ values at all j tested (see Table 2). The different rate of PX decay was then much more apparent at times > 30 min, once the oxidizing hydroxyl radicals acted significantly on intermediates or were consumed in parasitic reactions. This caused the deceleration of pesticide removal, which was more significant at 100 mA cm^{-2} since greater amounts of these oxidants were produced.

The consumption of BDD($^{\bullet}$OH) and $^{\bullet}$OH in parasitic reactions was verified by determining the MCE values of the runs shown in Fig. 5a. As can be seen in Fig. 5b, the current efficiency always dropped when prolonging electrolyses due to the removal of organic matter and the generation of more recalcitrant products, as stated above. Moreover, the MCE values underwent a progressive fall at higher j, despite the greater TOC abatement, at least between 33.3 and 66.6 mA cm^{-2} (see Fig. 5a), as expected from the waste of the excess of hydroxyl radicals. Examples of such reactions include the oxidation of BDD($^{\bullet}$OH) to O_2 via reaction (9) and the destruction of $^{\bullet}$OH by Fe^{2+} and H_2O_2 via reactions (10) and (11), respectively (Özcan et al. 2008; Sirés and Brillas 2012; Sirés et al. 2014). Furthermore, Panizza and Cerisola (2009), when reviewing the oxidation characteristics of the BDD anode, remarked the increase in rate of other anode reactions originating weaker oxidants like ozone by reaction (12) and $S_2O_8^{2-}$ ion from SO_4^{2-} ion by reaction (13) as j was raised, eventually inhibiting the H_2O discharge from reaction (1).

$$2BDD(^{\bullet}OH) \rightarrow 2BDD + O_2 + 2H^+ + 2e^- \tag{9}$$

$$Fe^{2+} + {}^{\bullet}OH \rightarrow Fe^{3+} + OH^- \tag{10}$$

$$H_2O_2 + {}^{\bullet}OH \rightarrow HO_2^{\bullet} + H_2O \tag{11}$$

15

1     $3H_2O \rightarrow O_3 + 6H^+ + 6e^-$ (12)

2     $2SO_4^{2-} \rightarrow S_2O_8^{2-} + 2e^-$ (13)

3   Based on the aforementioned considerations, the highest current efficiency was attained

4 at the lowest j of 33.3 mA cm^{-2}, yielding a highest value of 14.0% at 30 min (see Table 2).

5 Effect of iron ions on the EF and PEF processes

6   Another important parameter in the Fenton systems is the amount of iron ions acting as

7 catalyst because they control the $^\bullet$OH production from Fenton's reaction (3) as well as the

8 generation of Fe(II) and/or Fe(III) complexes of organic compounds. To study this influence,

9 0.38 mM PX solutions in 0.05 M Na$_2$SO$_4$ with 0.10-1.50 mM Fe^{2+} at pH 3.0 were treated by

10 EF at $j = 100$ mA cm^{-2} and 25 ºC. The concentration decay for these trials is depicted in Fig.

11 6a. The increase in Fe^{2+} concentration caused a quicker pesticide decay, which was

12 completely removed at shorter times of 240, 120, 105 and 20 min at 0.10, 0.50, 1.00 and 1.50

13 mM Fe^{2+}, respectively. A detailed kinetic analysis of the pseudo-first-order profiles confirmed

14 the presence of two-consecutive regions at 0.50 and 1.00 mM Fe^{2+}, whereas only a single

15 linear correlation was found at 0.10 and 1.50 mM (see the inset panel of Fig. 6a). From the

16 corresponding apparent rate constants given in Table 2, one can infer an average $k_{app,1}$ value

17 of 0.158 ± 0.017 min^{-1} at 0.50, 1.00 and 1.50 mM Fe^{2+}. This is indicative of a rapid oxidation

18 of the same species by $^\bullet$OH in this region, which can be rather related to the formation of

19 Fe(II)-PX complexes because they are favored at high Fe^{2+} content like 1.50 mM. In contrast,

20 the much smaller $k_{app,1}$ value at 0.10 mM Fe^{2+} was of the same order of magnitude as the $k_{app,2}$

21 ones obtained at 0.50 and 1.00 mM Fe^{2+}, although these values grew as Fe^{2+} content raised.

22 This finding confirms that Fe(III)-PX complexes are removed in that region, more rapidly at

23 higher Fe^{2+} concentration because of the greater $^\bullet$OH generation. The single pseudo-first-

1   order profile found at the lowest Fe^{2+} content of 0.10 mM can be related to the preponderance

2   of the Fe(III)-PX species alone due to the rapid conversion of Fe^{2+} to Fe^{3+} via Fenton's

3   reaction (3).

4   As for the mineralization in the above trials, Fig. 6b highlights a slower TOC reduction at

5   0.10 mM Fe^{2+}, reaching 87% mineralization owing to the small production of additional $^{\bullet}OH$.

6   Fig. 6b also shows that the quicker TOC removal at 0.50 mM Fe^{2+} was upgraded during the

7   first 120 min using 1.00 and 1.50 mM Fe^{2+}, whereupon it decayed at similar rate for all these

8   Fe^{2+} concentrations up to attain 90-92% mineralization at 540 min (see Table 2). Under such

9   conditions, one can presume that similar amounts of intermediates were destroyed by

10   analogous quantities of BDD($^{\bullet}OH$) and $^{\bullet}OH$. The corresponding MCE values for these trials

11   always decreased from 30 to 540 min, as deduced from the data of Table 2. These results

12   allow concluding that 0.50 mM can be chosen as the minimal, optimal Fe^{2+} concentration for

13   EF and PEF processes because it yields the maximal mineralization degree.

14   To corroborate the complex PX decay kinetics in the presence of Fe^{3+} ion, a comparative

15   PEF experiment was made by degrading a 0.38 mM pesticide solution with 0.50 mM Fe^{3+} at

16   pH 3.0 and $j = 100$ mA cm^{-2}. Fig. 7a reveals that, at the beginning, the removal of PX was

17   strongly hampered using Fe^{3+} as catalyst compared to Fe^{2+}, although in both cases its total

18   disappearance occurred at 60 min. This can be accounted for by the initial formation of

19   Fe(III)-PX species that are removed by BDD($^{\bullet}OH$) and $^{\bullet}OH$. The oxidation of this species

20   also occurs using Fe^{2+}, thus decelerating the degradation process at times > 5 min, when this

21   ion has been largely transformed into Fe^{3+}. This behavior can also be deduced from the

22   pseudo-first-order kinetic analysis performed for the above concentration decays and

23   presented in the inset panel of Fig. 7a. While two consecutive pseudo-first-order regions were

24   found when Fe^{2+} was added, which can be ascribed to the consecutive destruction of the

25   Fe(II) and Fe(III) complexes of PX, a single region was found in the presence of Fe^{3+}, with a

1 $k_{app,1}$ value close to that of $k_{app,2}$ using Fe^{2+} (see Table 2). Note that the pseudo-first-order

2 profiles for these trials can only be fitted for short times up to 20-25 min, since at longer time

3 the kinetic decay became much more complex due to the simultaneous removal of the

4 oxidation products. On the other hand, Fig. 7b shows a rapid TOC abatement under PEF with

5 Fe^{3+}, reaching 89% mineralization at 420 min. This process was slower than PEF with Fe^{2+},

6 where total mineralization was achieved at that time, probably because less oxidant ($^\bullet$OH) was

7 originated from Fenton's reaction (3) as a result of the minor proportion of Fe^{2+} generated via

8 reaction (4). The lower oxidation power for PEF using Fe^{3+} instead of Fe^{2+} was also evident

9 from the lower MCE values obtained, as can be seen in Table 2.

10 Effect of substrate content on the EF treatment

11 Finally, the effect of the initial PX concentration on the performance of the EF process

12 was examined. This was made by treating 100 mL solutions containing from 0.19 to 0.76 mM

13 herbicide in 0.05 M Na_2SO_4 with the optimum 0.50 mM Fe^{2+} at pH 3.0, $j = 100$ mA cm^{-2} and

14 25 ºC for 540 min. No significant change in pH was found for these trials. Fig. 8 depicts a

15 gradually slower decay of the normalized concentration as the initial amount of PX was

16 raised, which can be simply ascribed to the less probable reaction with similar quantities of

17 BDD($^\bullet$OH) and $^\bullet$OH originated at the same j. Total removal of the pesticide was then

18 achieved after 90, 120 and 150 min for 0.19, 0.38 and 0.76 mM PX, respectively. The kinetic

19 analysis of these data is given in the inset panel of Fig. 8 and shows the existence of two

20 consecutive regions in all cases, although no good pseudo-first-order correlations were

21 determined for the first region of 0.19 and 0.76 mM. Regarding the second region, excellent

22 pseudo-first-order profiles were always obtained, with $k_{app,2}$ values very close to 0.016 min^{-1}

23 for 0.19 and 0.38 mM, which dropped to 0.008 min^{-1} for 0.76 mM due to the presence of

18

1   higher organic load. Again, this behavior was only found for times below 30 min, where no

2   significant interference from the degradation of intermediates occurs.

3   For the above assays, Fig. 9a highlights a similar normalized TOC removal, slightly

4   quicker for 0.76 mM PX after 180 min of electrolysis up to attain 95% mineralization at 540

5   min, a value similar to that determined for the other concentrations (see Table 2). Since a

6   greater amount of TOC was destroyed at a growing organic load, the EF process became more

7   efficient. This trend can be easily deduced from the MCE values given in Fig. 9b. The highest

8   current efficiency was achieved for 0.76 mM PX, varying from 9.0% at 30 min to 5.1% at 540

9   min (see Table 2). This means that organics are gradually attacked by greater amounts of

10   BDD($^\bullet$OH) and $^\bullet$OH coming from the deceleration of parasitic reactions (9)-(11). These

11   findings lead to conclude that the oxidation ability of EF and the powerful PEF is strongly

12   improved as the pesticide content increases.

13   Identification of primary products

14   Table 3 summarizes the four primary products detected by LC-MS that resulted from the

15   degradation of PX (**1**) during the EF treatment of a 0.38 mM pesticide solution with 0.50 mM

16   Fe^{2+} at pH 3.0 and j = 100 mA cm^{-2}. As can be seen, two aromatic products were identified.

17   While hydroxylation of the benzene ring of **1** yielded the compound **2**, the loss of its –NH-

18   CH$_3$ group led to the compound **3**.

19   **Conclusions**

20   It has been shown that the PEF process is the most powerful EAOP for the treatment of

21   water polluted with PX using a BDD/air-diffusion cell since it is able to completely

22   mineralize this pesticide thanks to the combined oxidative action of generated hydroxyl

23   radicals and UVA radiation. Partial mineralization with TOC removal above 90% was also

19

feasible by EF, whereas slightly poorer mineralization can be achieved by EO-H_2O_2. While a pseudo-first-order kinetics was determined for the pesticide abatement in EO-H_2O_2 owing to its reaction with BDD($^\bullet$OH), a rapid pseudo-first-order kinetics followed by a much slower one, related to the oxidation of its Fe(II) complexes by $^\bullet$OH and Fe(III) complexes by both BDD($^\bullet$OH) and $^\bullet$OH, respectively, was found in EF and PEF. The kinetic decay of PX and its final mineralization degree were practically independent of pH in EO-H_2O_2. In EF, an increase in j caused a quicker abatement of organics but with lower current efficiency because of the acceleration of parasitic reactions. An optimum concentration of 0.50 mM Fe^{2+} was determined for the EF process. Higher current efficiency with similar mineralization degree was also found by increasing substrate concentration. Two aromatic primary products were identified by LC-MS during the EF degradation of PX solutions.

Acknowledgments

References

ANVISA – Brazilian Health Surveillance Agency. Available from: <http://portal.anvisa.gov.br/wps/content/Anvisa+Portal/Anvisa/Inicio/Agrotoxicos+e+Toxicologia/Assuntos+de+Interesse/Monografias+de+Agrotoxicos/Monografias>, (last access: November 1, 2015).

APHA, Standard methods for the Examination of Water and Wastewater, 22th ed., American Public Health Association, New York, 2012.

Benítez FJ, Beltrán-Heredia J, González T (1995) Degradation of propoxur by ozone. J Environ Sci Health A 30(2):365-378. doi: 10.1080/10934529509376205.

Biziuk M, Przyjazny A, Czerwinski J, Wiergowski M (1996) Occurrence and determination of pesticides in natural and treated waters. J Chromatogr A 754(1-2):103-123. doi: 10.1016/S0021-9673(96)00297-X.

Borràs N, Oliver R, Arias C, Brillas E (2010) Degradation of atrazine by electrochemical advanced oxidation processes using a boron-doped diamond anode. J Phys Chem A 114(24):6613-6621. doi: 10.1021/jp1035647.

Brillas E, Martínez-Huitle CA (2015) Decontamination of wastewaters containing synthetic organic dyes by electrochemical methods. An updated review. Appl Catal B-Environ 166-167:603-643. doi: 10.1016/j.apcatb.2008.09.017.

Brillas E, Sirés I, Oturan MA (2009) Electro-Fenton process and related electrochemical technologies based on Fenton's reaction chemistry. Chem Rev 109(12):6570-6631. doi: 10.1021/cr900136g.

Cavalcanti EB, Garcia-Segura S, Centellas F, Brillas E (2013) Electrochemical incineration of omeprazole in neutral aqueous medium using a platinum or boron-doped diamond.

Degradation kinetics and oxidation products. Water Res 47(5):1803-1815. doi: 10.1016/j.watres.2013.01.002.

Ciríaco L, Anjo C, Correia J, Pacheco MJ, Lopes A (2009) Electrochemical degradation of ibuprofen on $Ti/Pt/PbO_2$ and Si/BDD electrodes. Electrochim Acta 54(5):1464-1472. doi: 10.1016/j.electacta.2008.09.022

Chiron S, Fernandez-Alba, AR, Rodriguez A, Garcia-Calvo E (2000) Pesticide chemical oxidation: State-of-the-art. Water Res 34(2):366-377. doi: 10.1016/S0043-1354(99)00173-6.

Cruz-González K, Torres-López O, García-León A, Brillas E, Hernández-Ramírez A, Peralta-Hernández JM (2012) Optimization of electro-Fenton/BDD process for decolorization of a model azo dye wastewater by means of response surface methodology. Desalination 286:63-68. doi: 10.1016/j.desal.2011.11.005.

Dirany A, Sirés I, Oturan N, Özcan A, Oturan MA (2012) Electrochemical treatment of the antibiotic sulfachloropyridazine: kinetics, reaction pathways, and toxicity evolution. Environ Sci Technol 46(7):4074-4082. doi: 10.1021/es204621q.

El-Ghenymy A, Rodríguez RM, Brillas E, Oturan N, Oturan MA (2014) Electro-Fenton degradation of the antibiotic sulfanilamide with Pt/carbon-felt and BDD/carbon-felt cells. Kinetics, reaction intermediates, and toxicity assessment. Environ Sci Pollut Res 21(14):8368-8378. doi: 10.1007/s11356-014-2773-3.

Florenza X, Solano AMS, Centellas F, Martínez-Huitle CA, Brillas E, Garcia-Segura S (2014) Degradation of the azo dye Acid Red 1 by anodic oxidation and indirect electrochemical processes based on Fenton's reaction chemistry. Relationship between decolorization, mineralization and products. Electrochim Acta 142:276-288. doi: 10.1016/j.electacta.2014.07.117.

22

1   Guinea E, Brillas E, Centellas F, Cañizares P, Rodrigo MA, Saez C (2009) Oxidation of enrofloxacin with conductive-diamond electrochemical oxidation, ozonation and Fenton oxidation. A comparison. Water Res 43(8):2131-2138. doi: 10.1016/j.watres.2009.02.025.

Gozzi F, Machulek Jr A, Ferreira VS, Osugi ME, Santos APF, Nogueira JA, Dantas RF, Esplugas S, Oliveira SC (2012) Investigation of chlorimuron-ethyl degradation by Fenton, photo-Fenton and ozonation process. Chem Eng J 210: 444-450. doi: 10.1016/j.cej.2012.09.008.

Hatchard CG, Parker CA (1956) A new sensitive chemical actinometer II. Potassium ferrioxalate as a standard chemical actinometer. P R Soc A, pp. 518-536. doi: 10.1098/rspa.1956.0102.

Isarain-Chávez E, Arias C, Cabot PL, Centellas F, Rodriguez RM, Garrido JA, Brillas E (2010) Mineralization of the drug beta-blocker atenolol by electro-Fenton and photoelectro-Fenton using an air-diffusion cathode for H_2O_2 electrogeneration combined with a carbon-felt cathode for Fe^{2+} regeneration. Appl Catal B-Environ 96(3-4):361-369. doi: 10.1016/j.apcatb.2010.02.033.

Khataee A, Akbarpour A, Vahi B (2014) Photoassisted electrochemical degradation of an azo dye using Ti/RuO_2 anode and carbon nanotubes containing gas-diffusion cathode. J Taiwan Inst Chem Eng 45(3):930-936. doi: 10.1016/j.jtice.2013.08.015.

Klavarioti M, Mantzavinos D, Kassinos D (2009) Removal of residual pharmaceuticals from aqueous systems by advanced oxidation processes. Environ Int 35(2):402-417. doi: 10.1016/j.envint.2008.07.009

Lu, MC, Chen JN, Chang KT (1999) Effect of adsorbents coated with titanium dioxide on the photocatalytic degradation of propoxur. Chemosphere 38(3):617-627. doi: 1016/S0045-6535(98)00204-5.

23

1 Machulek Jr A, Gogritcchiani E, Moraes JEF, Quina FH, Braun AM, Oliveros E (2009)

2 Kinetic and mechanistic investigation of the ozonolysis of 2,4-xylidine (2,4-dimethyl-

3 aniline) in acid aqueous solution. Sep Purif Technol 67(2):141-148. doi:

4 1016/j.seppur.2009.03.024.

5 Machulek Jr A, Oliveira SC, Osugi ME, Ferreira VS, Quina FH, Dantas RF, Oliveira SL,

6 Casagrande GA, Anaissi FJ, Silva VO, Cavalcante RP, Gozzi F, Ramos DD, Rosa APP,

7 Santos APF, Castro DC, Nogueira JA (2013) Application of different advanced

8 oxidation processes for the degradation of organic pollutants. In: Rashed MM (ed)

9 Organic Pollutants - Monitoring, Risk and Treatment. Rijeka: InTech, pp. 141-166. doi:

10 10.5772/53188

11 Mahalakshmi M, Priya SV, Arabindoo B, Murugesan PV (2009) Photocatalytic degradation

12 of aqueous propoxur solution using TiO_2 and Hβ zeolite-supported TiO_2. J Hazard

13 Mater 161(1):336-343. doi: 10.1016/j.jhazmat.2008.03.098.

14 Marselli B, Garcia-Gomez J, Michaud PA, Rodrigo MA, Comninellis C (2003)

15 Electrogeneration of hydroxyl radicals on boron-doped diamond electrodes. J

16 Electrochem Soc 150(3):D79-D83. doi: 10.1149/1.1553790.

17 Martínez-Huitle CA, Ferro S (2006) Electrochemical oxidation of organic pollutants for the

18 wastewater treatment: Direct and indirect processes. Chem Soc Rev 35(12):1324-1340.

19 doi: 10.1039/B517632H.

20 Moreira FC, Garcia-Segura S, Vilar VJP, Boaventura RAR, Brillas E (2013) Decolorization

21 and mineralization of Sunset Yellow FCF azo dye by anodic oxidation, electro-Fenton,

22 UVA photoelectro-Fenton and solar photoelectro-Fenton processes. Appl Catal B-

23 Environ 142-143:877-890. doi: 10.1016/j.apcatb.2013.03.023.

Özcan A, Şahin Y, Oturan MA (2008) Removal of propham from water by using electro-Fenton technology: Kinetics and mechanism. Chemosphere 73(5):737-744. doi: 10.1016/j.chemosphere.2008.06.027.

Pandey MR, Guo H (2014) Evaluation of cytoxicity, genotoxicity and embryotoxicity of insecticide propoxur using flounder gill (FG) cells and zebrafish embryos. Toxicol Vitro 28(3):340-353. doi: 10.1016/j.tiv.2013.11.010.

Panizza M, Cerisola G (2009) Direct and mediated anodic oxidation of organic pollutants. Chem Rev 109(12):6541-6569. doi: 10.1021/cr9001319.

Pérez-Ruiz T, Martínez-Lozano C, García MD (2007) Determination of propoxur in environmental samples by automated solid-phase extraction followed by flow-injection analysis with tris (2,2-bipyridyl) ruthenium (II) chemiluminescence detection. Anal Chim Acta 584(2):275-280. doi: 10.1016/j.aca.2006.11.062.

Pimentel D (1996) Green revolution agriculture and chemical hazards. Sci Total Environ 188(2-3):86-98. doi: 10.1016/0048-9697(96)05280-1.

Ramos DD, Bezerra PC, Quina FH, Dantas RF, Casagrande GA, Oliveira SC, Oliveira MRS, Oliveira LCS, Ferreira VS, Oliveira SL, Machulek Jr A (2015) Synthesis and characterization of TiO_2 and TiO_2/Ag for use in photodegradation of methylviologen, with kinetics study by laser flash photolysis. Environ Sci Pollut Res 22(2):774-783. doi: 10.1007/s11356-014-2678-1.

Rao YF, Chu W (2010) Degradation of linuron by UV, ozonation, and UV/O_3 processes – Effect of anions and reaction mechanism. J Hazard Mater 180(1-3):514-523. doi: 10.1016/j.jhazmat.2010.04.063.

Reddy PVL, Kim KH (2015) A review of photochemical approaches for the treatment of a wide range of pesticides. J Hazard Mater 285:325-335. doi: 10.1016/j.jhazmat.2014.11.036.

1   Rodrigo MA, Cañizares P, Sánchez-Carretero A, Sáez C (2010) Use of conductive-diamond

2   electrochemical oxidation for wastewater treatment. Catal Today 151(1-2):173-177. doi:

3   10.1016/j.cattod.2010.01.058.

4   Rodrigo MA, Oturan N, Oturan MA (2014) Electrochemically assisted remediation of

5   pesticides in soils and water: A review, Chem Rev 114(17):8720–8745. doi:

6   10.1021/cr500077e.

7   Ruiz EJ, Hernández-Ramírez A, Peralta-Hernández JM, Arias C, Brillas E (2011) Application

8   of solar photoelectro-Fenton technology to azo dyes mineralization: Effect of current

9   density, Fe^{2+} and dye concentrations. Chem Eng J 171(2):385-392. doi:

10   10.1016/j.cej.2011.03.004

11   Sanjuán A, Aguirre G, Álvaro M, García H, Scaiano JC (2000) Degradation of propoxur in

12   water using 2, 4, 6-triphenylpyrylium–Zeolite Y as photocatalyst: Product study and

13   laser flash photolysis. Appl Catal B-Environ 25(4):257-265. doi: 10.1016/S0926-

14   3373(99)00140-X.

15   Sirés I, Brillas, E (2012) Remediation of water pollution caused by pharmaceutical residues

16   based on electrochemical separation and degradation technologies: a review. Environ

17   Int 40:212-229. doi: 10.1016/j.envint.2011.07.012.

18   Sirés I, Brillas E, Oturan MA, Rodrigo MA, Panizza M (2014) Eletrochemical advanced

19   oxidation processes: today and tomorrow. A review. Environ Sci Pollut Res

20   21(14):8336-8367. doi: 10.1007/S11356-014-2783-1.

21   Soares AFS, Leão MMD, de Faria VHF, da Costa MCM, Moura ACM, Ramos VDV, Neto

22   MRV, da Costa EP (2013) Occurrence of pesticides from coffee crops in surface water.

23   Ambi-Agua 8(1):62-72. doi: 10.4136/ambi-agua.1053.

24   Sun L, Lee HK (2003) Stability studies of propoxur herbicide in environmental water samples

25   by liquid chromatography – atmospheric pressure chemical ionization ion-trap mass

26

spectrometry. J Chromatogr A 1014(1-2):153-163. doi: 10.1016/S0021-9673(03)00850-1.

Thiam A, Brillas E, Garrido JA, Rodriguez RM, Sirés I (2016) Routes for the electrochemical degradation of the artificial food azo-colour Ponceau 4R by advanced oxidation processes. Appl Catal B: Environ 180:227-236. doi: 10.1016/j.apcatb.2015.06.039.

Thiam A, Sirés I, Centellas F, Cabot PL, Brillas E (2015) Decolorization and mineralization of Allura Red AC azo dye by solar photoelectro-Fenton: Identification of intermediates. Chemosphere 136:1-8. doi: 10.1016/j.chemosphere.2015.03.047.

Thiam A, Zhou M, Brillas E, Sirés I (2014) Two-step mineralization of Tartrazine solutions: Study of parameters and by-products during the coupling of electrocoagulation with electrochemical advanced oxidation processes. Appl Catal B-Environ 150-151:116-125. doi: 10.1016/j.apcatb.2013.12.011.

Vasudevan S, Oturan MA (2014) Electrochemistry: As cause and cure in water pollution-an overview. Environ Chem Lett 12(1):97-108. doi: 10.1007/s10311-013-0434-2.

Vatanpour V, Daneshvar N, Rasoulifard MH (2009) Electro-Fenton degradation of synthetic dye mixture: influence of intermediates. J Environ Eng Manage 19(5):277-282.

WHO - World Health Organization. 2003. "WHO Specifications and evaluations for public health pesticides." Propoxur: (2-isopropoxyphenyl methylcarbamate)", pp. 1-25.

Yahya MS, Oturan N, El Kacemi K, El Karbane M, Aravindakumar CT, Oturan MA (2014) Oxidative degradation study on antimicrobial agent ciprofloxacin by electro-Fenton process: Kinetics and oxidation products. Chemosphere 117:447-454. doi: 10.1016/j.chemosphere.2014.08.016.

1 **Figure captions**

2 **Fig. 1** Propoxur (PX) concentration decay with electrolysis time for the degradation of 100

3 mL of 0.38 mM insecticide solutions in 0.05 M Na_2SO_4 at pH 3.0 and 25 ºC using an open

4 and undivided cell with a 3 cm^2 boron-doped diamond (BDD) anode and 3 cm^2 air-diffusion

5 cathode at 100 mA cm^{-2}. Method: (O) electrochemical oxidation with electrogenerated H_2O_2

6 (EO-H_2O_2), ($\square$) electro-Fenton (EF) with 0.50 mM Fe^{2+} and ($\blacktriangle$) photoelectro-Fenton (PEF)

7 with 0.50 mM Fe^{2+} under 4 W UVA irradiation. The inset panel presents the corresponding

8 kinetic analysis assuming that PX follows a pseudo-first-order reaction. The time scale has

9 been shortened to remark the kinetics in EF and PEF.

10 **Fig. 2** Change of (a) TOC removal and (b) mineralization current efficiency with electrolysis

11 time for the trials shown in Fig. 1.

12 **Fig. 3** Effect of pH on (a) propoxur concentration decay and (b) TOC removals vs.

13 electrolysis time for the EO-H_2O_2 treatment of 100 mL of 0.38 mM insecticide solutions in

14 0.05 M Na_2SO_4 at 100 mA cm^{-2} and 25 ºC. Initial pH: (O) 3.0, ($\diamond$) 5.0 and ($\triangle$) 9.0. The

15 kinetic analysis considering a pseudo-first-order reaction for propoxur is given in the inset

16 panel of plot (a).

17 **Fig. 4** Effect of current density on propoxur content abatement with electrolysis time for the

18 EF degradation of 100 mL of a 0.38 mM insecticide solution in 0.05 M Na_2SO_4 with 0.50 mM

19 Fe^{2+} at pH 3.0 and 25 ºC. Current density: ($\triangledown$) 33.3 mA cm^{-2}, ($\square$) 66.7 mA cm^{-2} and (O) 100

20 mA cm^{-2}. The inset panel gives the corresponding kinetic analysis assuming a pseudo-first-

21 order reaction for propoxur.

22 **Fig. 5** (a) TOC decay and (b) mineralization current efficiency vs. electrolysis time for the

23 experiments of Fig. 4.

28

1   **Fig. 6** Effect of Fe^{2+} concentration on (a) propoxur content decay and (b) TOC abatement

2   with electrolysis time for the EF treatment of 100 mL of 0.38 mM insecticide solutions in

3   0.05 M Na_2SO_4 at pH 3.0, 100 mA cm^{-2} and 25 ºC. Fe^{2+} concentration: ($\diamond$) 0.10 mM, ($\bigcirc$)

4   0.50 mM, ($\square$) 1.00 mM and ($\triangle$) 1.50 mM. The inset panel depicts the corresponding kinetic

5   analysis assuming a pseudo-first-order reaction for propoxur.

6   **Fig. 7** Influence of Fe catalyst on (a) propoxur concentration abatement and (b) TOC removal

7   with electrolysis time for the PEF degradation of 100 mL of a 0.38 mM insecticide solution in

8   0.05 M Na_2SO_4 at pH 3.0, 100 mA cm^{-2} and 25 ºC. Iron concentration: ($\blacktriangle$) 0.50 mM Fe^{2+} and

9   ($\blacksquare$) 0.50 mM Fe^{3+}. The kinetic analysis considering that propoxur obeys a pseudo-first-order

10   reaction is shown in the inset panel.

11   **Fig. 8** Effect of initial insecticide concentration on its normalized decay vs. electrolysis time

12   for the EF treatment of 100 mL of propoxur solutions in 0.05 M Na_2SO_4 with 0.50 mM Fe^{2+}

13   at pH 3.0, 100 mA cm^{-2} and 25 ºC. Propoxur concentration: ($\triangle$) 0.19 mM, ($\bigcirc$) 0.38 mM and

14   ($\triangledown$) 0.76 mM. The inset panel gives the kinetic analysis for a pseudo-first-order reaction of

15   the insecticide.

16   **Fig. 9** Variation of (a) normalized TOC abatement and (b) mineralization current efficiency

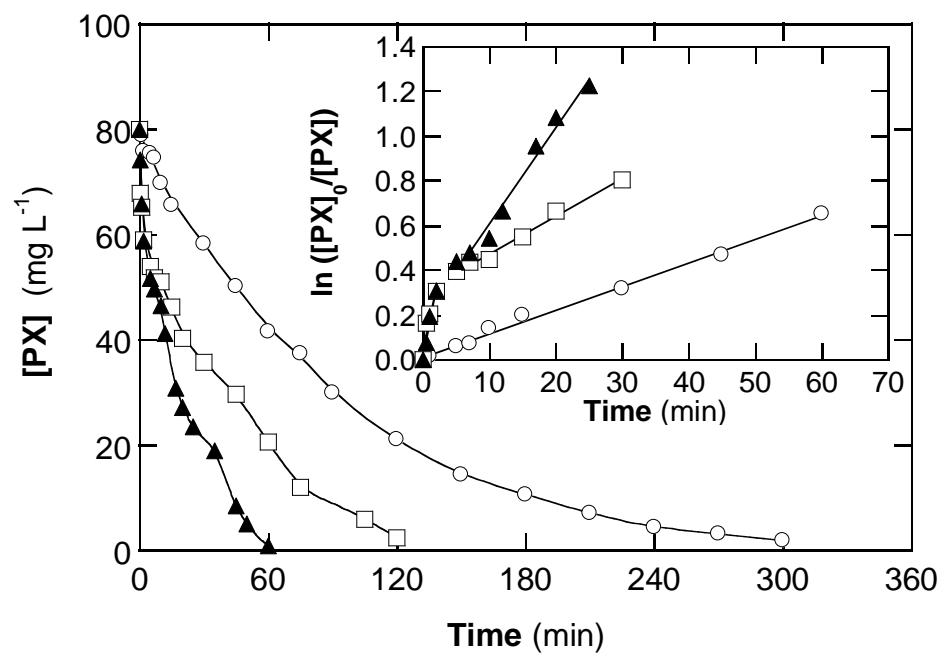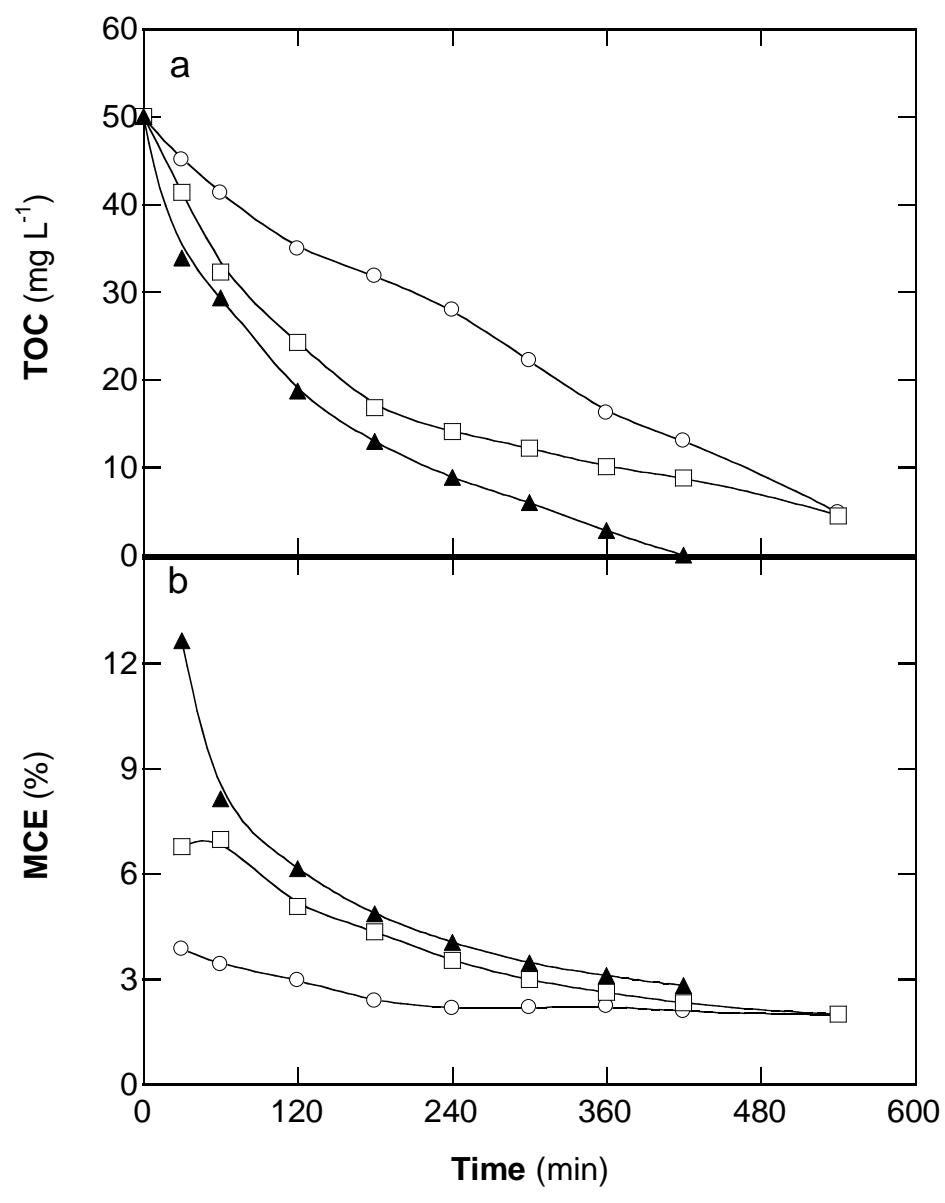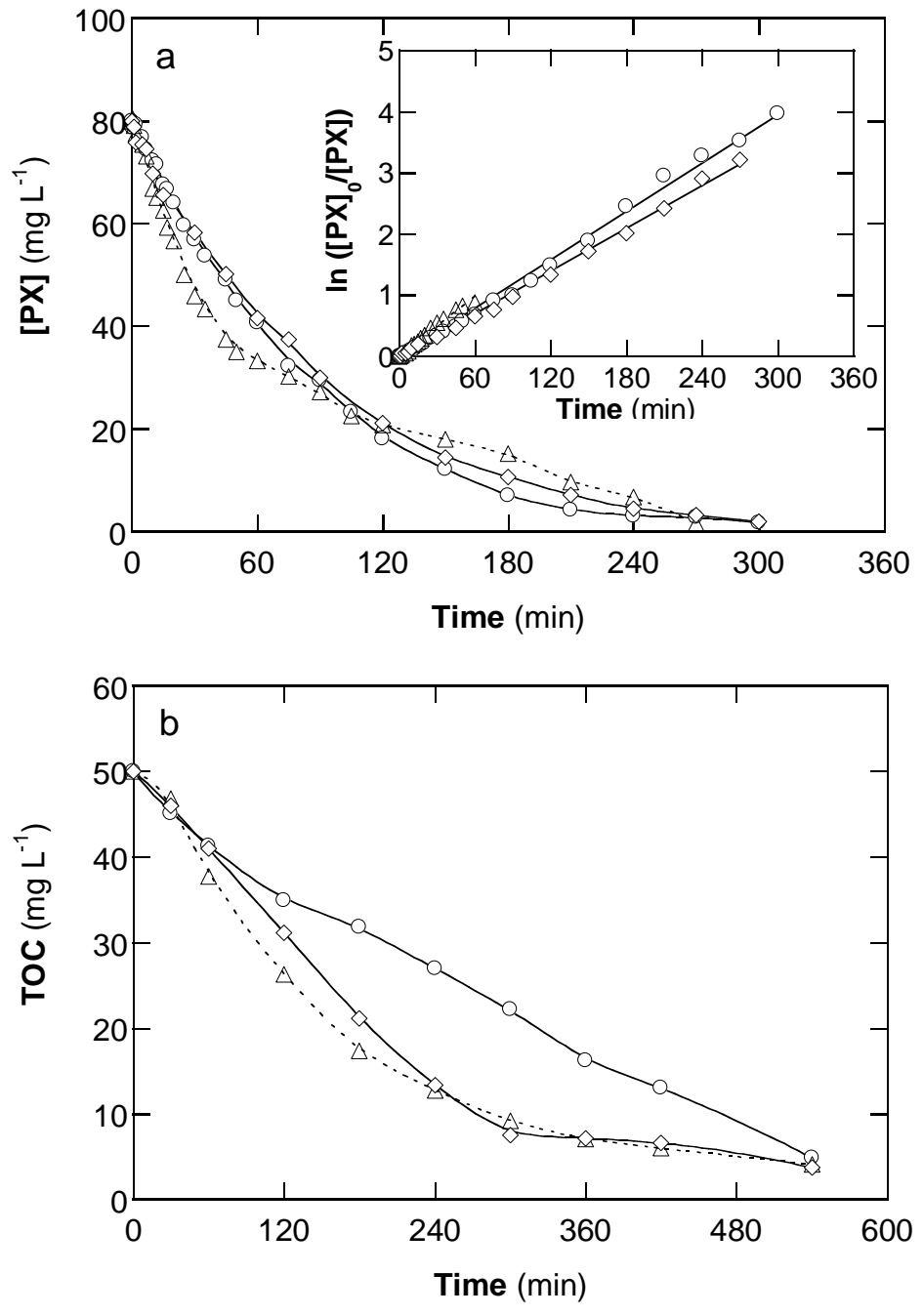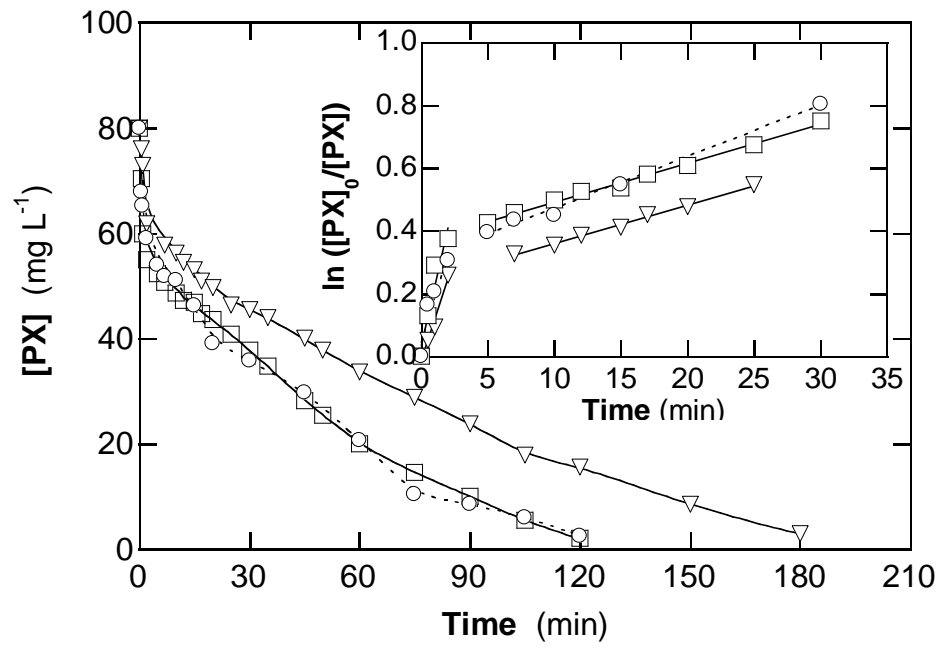17   with electrolysis time for the assays of Fig 8.

18

Figure 1

Fig. 1

Figure 2

Fig. 2

1

Figure 3

Fig. 3

Figure 4

Fig. 4

Figure 5

Fig. 5

1

Figure 6

Fig. 6

Figure 7

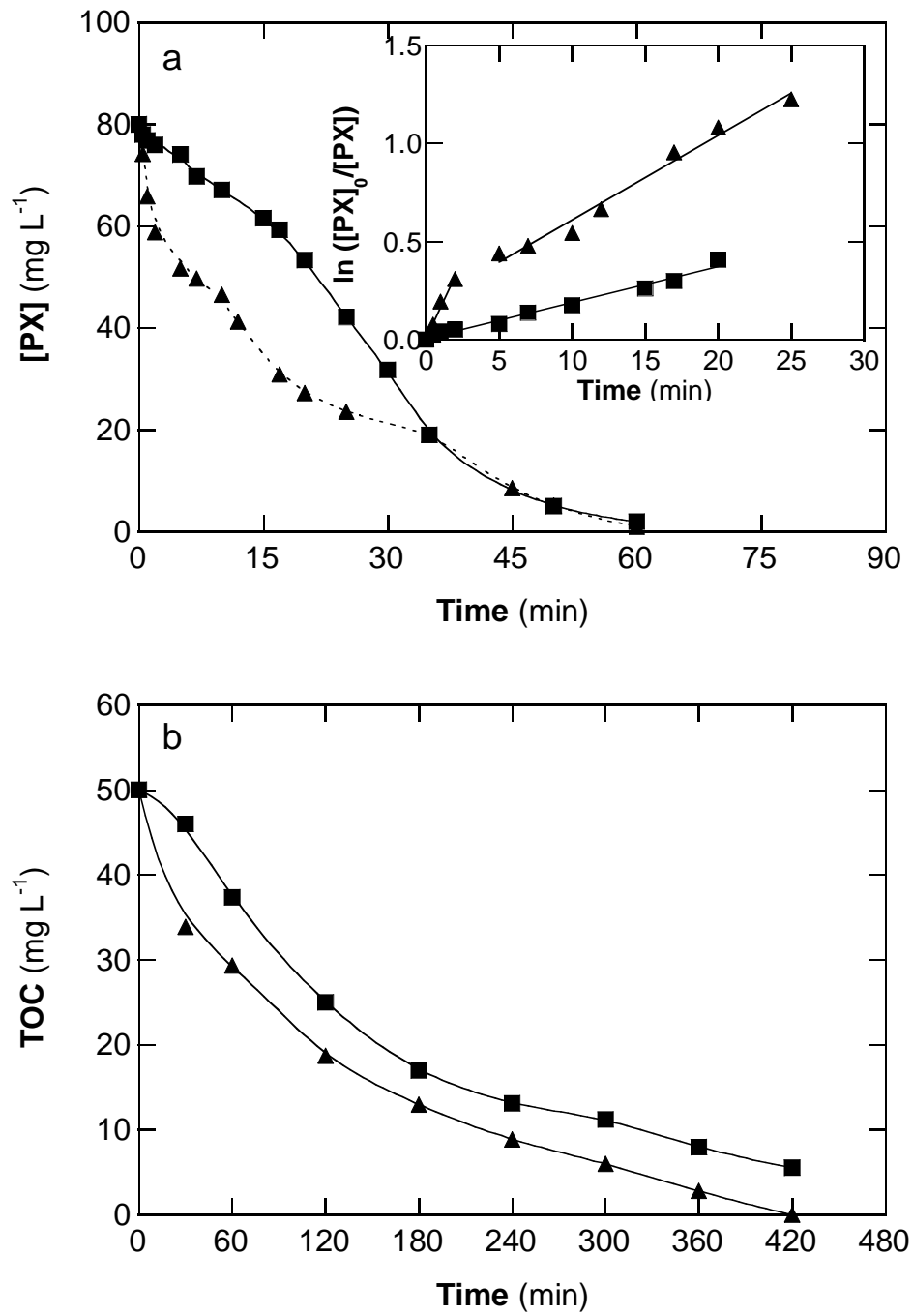
Fig. 7
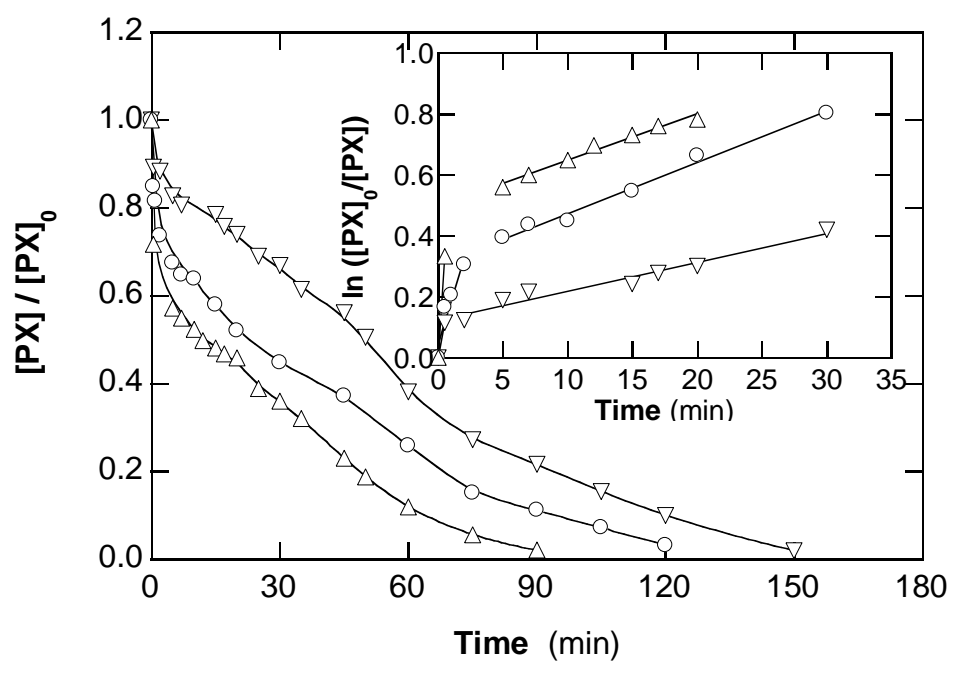
1
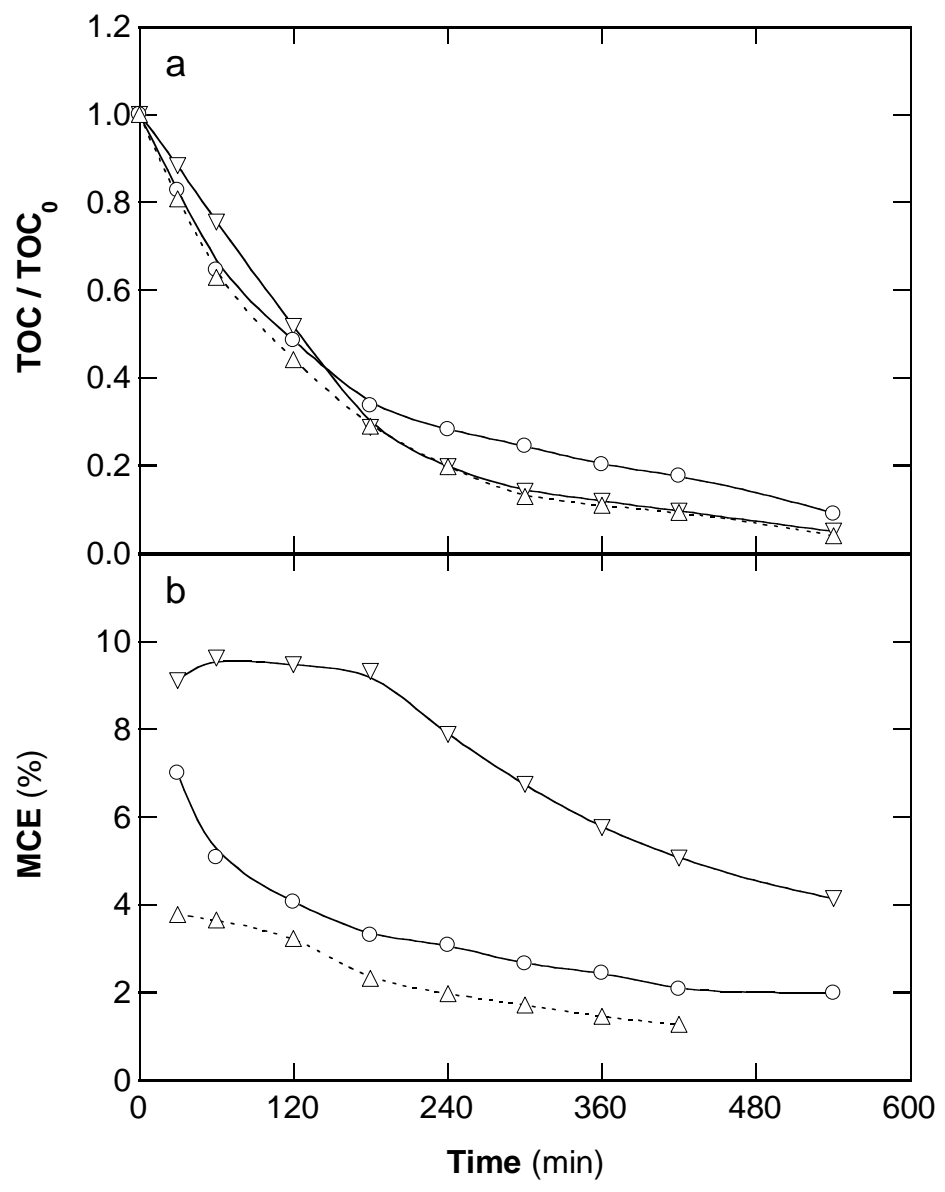
Figure 8

Fig. 8

1

Figure 9

Fig. 9

1
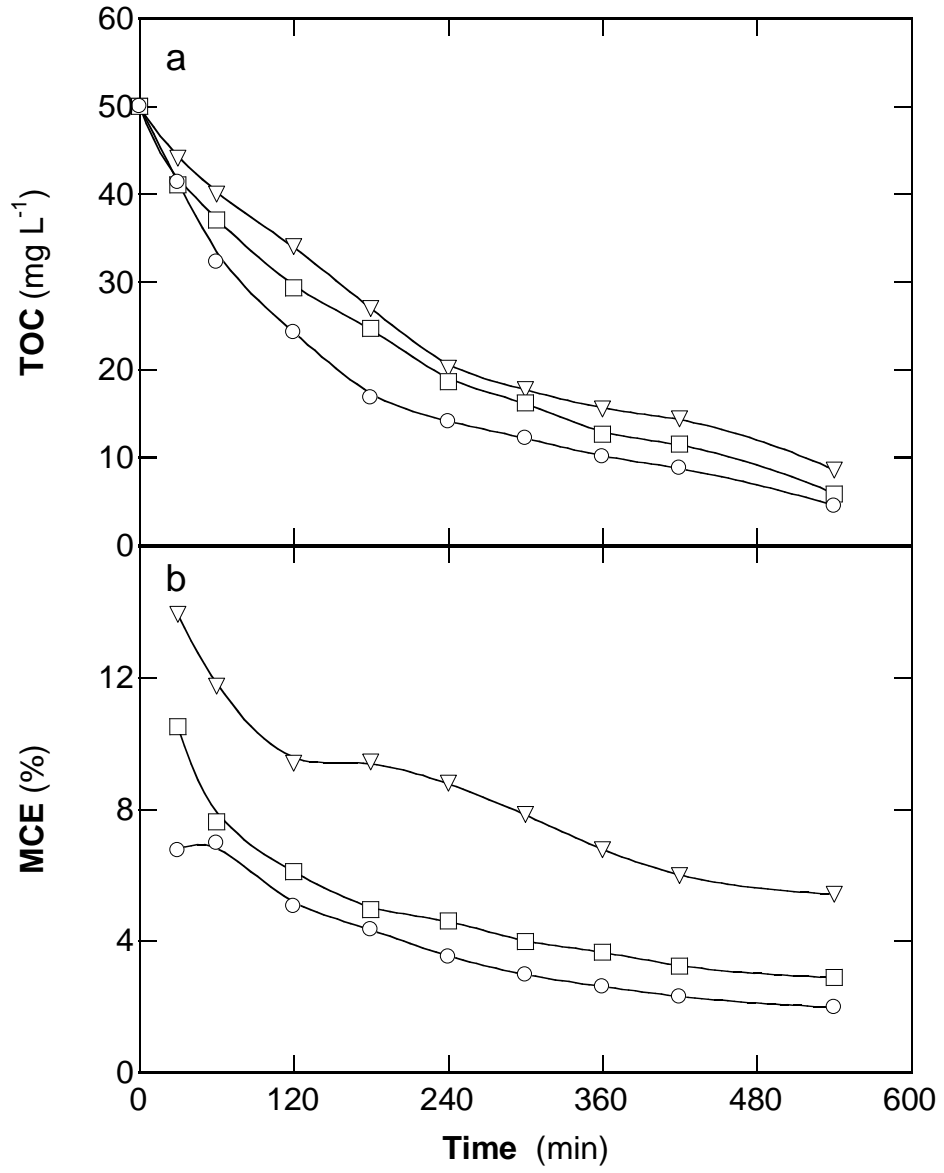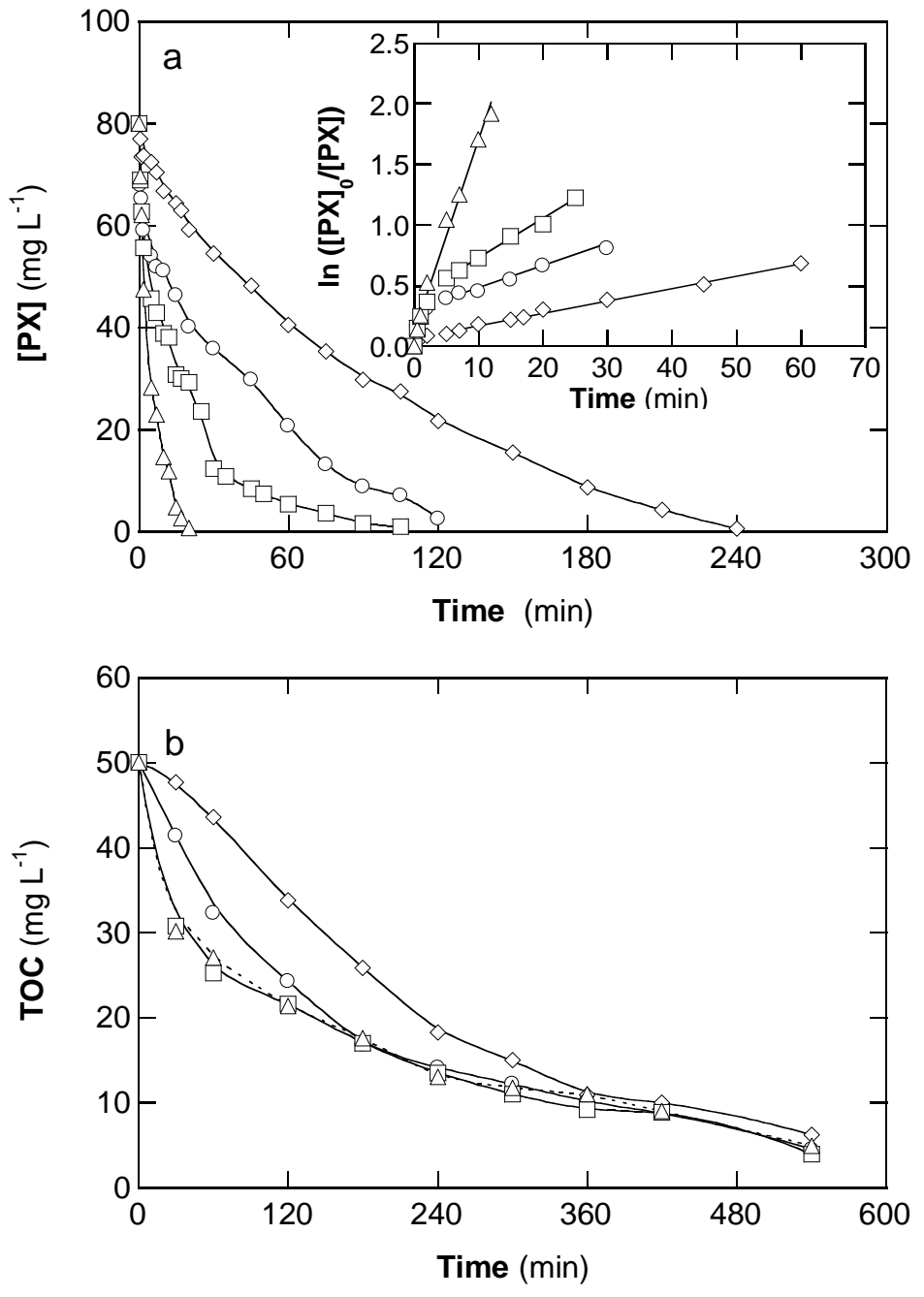
Table 1

Table 1 Results for the degradation of 100 mL of solutions containing 0.38 mM propoxur in 0.05 M Na_2SO_4 at different pH values by EO-H_2O_2 using a stirred BDD/air-diffusion cell at 100 mA cm^{-2} and 25 ℃

pH	k_{app} [a] (min^{-1})	R^2	% PX removal (t in min)	% TOC removal (t in min)	% MCE (at 30 min)	% MCE (at 420 min)
3.0	0.011	0.999	98 (300)	90 (540)	3.8	2.1
5.0	0.010	0.997	98 (300)	90 (540)	3.8	2.3
9.0	0.017	0.997	98 (300)	90 (540)	3.7	2.3

[a] k_{app}: apparent rate constant

Table 2

Table 2 Conditions and results for the degradation of 100 mL of solutions containing propoxur (PX) in 0.05 M Na_2SO_4 at 25 ℃ by different EF and PEF processes using a stirred BDD/air-diffusion cell

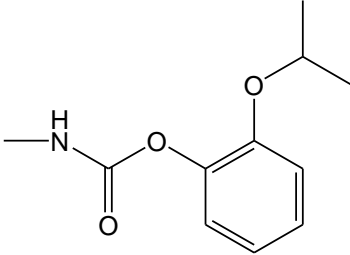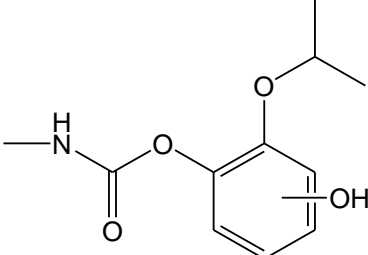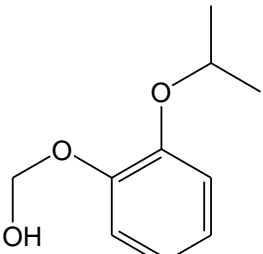| Method	[PX] (mM)	[Fe^{2+}] (mM)	j [a] (mA cm^{-2})	$k_{app,1}$ [b] (min^{-1})	R^2_1	$k_{app,2}$ [c] (min^{-1})	R^2_2	% PX removal (t in min)	% TOC removal (t in min)	% MCE (at 30 min)	% MCE (at 420 min)
EF	0.38	0.10	100	0.010	0.996	-	-	99 (240)	87 (540)	1.9	2.2
	0.38	0.50	100	0.141	0.975	0.016	0.986	97 (120)	91 (540)	6.7	2.3
	0.38	1.00	100	0.175	0.974	0.032	0.990	99 (105)	90 (540)	14.3	2.3
	0.38	1.50	100	0.158	0.993	-	-	99 (20)	92 (540)	14.9-	2.3
	0.38	0.50	33.3	0.130	0.978	0.012	0.997	96 (180)	83 (540)	14.0	6.0
	0.38	0.50	66.7	0.187	0.977	0.012	0.996	97 (120)	88 (540)	10.4	3.2
	0.19	0.50	100	-	-	0.015	0.988	98 (90)	96 (540)	3.7	1.3
	0.76	0.50	100	-	-	0.008	0.986	98 (150)	95 (540)	9.0	5.1
PEF	0.38	0.50 [d]	100	0.018	0.991	-	-	97 (60)	89 (420)	3.1	2.4
	0.38	0.50	100	0.157	0.989	0.043	0.990	99 (60)	100 (420)	12.6	2.8

[a] Current density

[b] $k_{app,1}$: apparent rate constant of single or first region

[c] $k_{app,2}$: apparent rate constant of second region

[d] Fe^{3+} concentration

Table 3

Table 3 Primary products identified by LC-MS after 5 and 90 min of EF degradation of 100 mL of a 0.38 mM propoxur solution in 0.05 M Na_2SO_4 with 0.50 mM Fe^{2+} of pH 3.0 using a stirred BDD/air-diffusion cell at 100 mA cm^{-2}

Compound	Molecular structure	Retention time (min)	m/z
1		13.24	210
2		9.11	226
3		8.98	183

1